processes

MDPI

Article

Liquid-Phase Removal of Methylene Blue as Organic Pollutant by Mesoporous Activated Carbon Prepared from Water Caltrop Husk Using Carbon Dioxide Activation

Yu-Quan Lin and Wen-Tien Tsai *

Graduate Institute of Bioresources, National Pingtung University of Science and Technology, Pingtung 912, Taiwan; wsx55222525@gmail.com

* Correspondence: wttsai@mail.npust.edu.tw; Tel.: +886-877-032-02

Abstract: In this work, a mesoporous activated carbon (AC) was prepared from a unique lignocellulosic biomass (water caltrop husk) in triplicate using a single-step physical activation process at lower temperature (i.e., 750 °C) and longer holding time (i.e., 90 min). Based on the pore properties and adsorption properties for removal of methylene blue (MB) as organic pollutant, the results proved that the resulting AC possesses a mesoporous feature with the Brunauer–Emmett–Teller (BET) surface area of 810.5 m^2/g and mesopore volume of about 0.13 cm^3/g. Due to its fast adsorption rate and maximal adsorption capacity fitted (126.6 mg/g), the mesoporous carbon material could be used as an excellent adsorbent for liquid-phase removal of MB. In addition, the pseudo-second-order model is well suited for describing the adsorption system between the cationic adsorbate and the resulting AC with oxygen surface groups.

Keywords: water caltrop husk; CO_2 activation; mesoporous activated carbon; methylene blue; adsorptive removal; kinetic modeling

Citation: Lin, Y.-Q.; Tsai, W.-T. Liquid-Phase Removal of Methylene Blue as Organic Pollutant by Mesoporous Activated Carbon Prepared from Water Caltrop Husk Using Carbon Dioxide Activation. *Processes* **2021**, *9*, 238. https://doi.org/10.3390/pr9020238

Academic Editor: Andrea Petrella

Received: 31 December 2020

Accepted: 25 January 2021

Published: 27 January 2021

1. Introduction

Organic chemicals (e.g., dyes, pesticides) released from anthropogenic activities have caused serious environmental issues because these pollutants have deteriorated the environmental quality in water, groundwater and soil phases. Furthermore, exposure to them will increase the health risks in both the food chain and drinking water. Therefore, many advanced treatment methods for the removal of organic pollutants from aqueous solutions have been developed in recent years [1]. Among these processes, activated carbon (AC) adsorption may be the most used method for the rapid removal of environmental pollutants from their existing phase (gas or liquid). An adsorption results in the removal of adsorbate molecules from the solution by diffusing them into porous adsorbent due to the concentration difference between the liquid and solid phases. Eventually, the concentration of the adsorbate remained in the solution will be in a dynamic equilibrium with that on the solid phase. In general, this recuperative process has significant features, including easy operation, low energy consumption, simple design, and high efficiency [2,3]. However, it should be noted that the adsorption process may be an expensive method due to the relatively high costs involved in commercial AC and its disposal, particularly when exhausted and not regenerated by steam for hydrolyzable adsorbates [4]. In this regard, there are many review papers focusing on the preparation of biomass-based AC and its applications for the removal of toxic pollutants from water in recent years [5–11]. The motivations for reusing agricultural residues as AC precursors also include sustainable waste management and climate change mitigation. On one hand, AC is usually a microporous carbonaceous material with high adsorption capacity [12], which is related to its specific surface area, pore volume, pore size distribution, and internal porosity [13]. However, the microporous feature in the AC materials could limit or restrict the transport diffusion of large molecule

adsorbates into the micropores with pore widths (or diameters) less than 2.0 nm [14], thus reducing the adsorption capacity and retarding the adsorption rate for reaching adsorption equilibrium [15,16]. To mitigate from the so-called wall effect, many studies have focused on the production of biomass-based AC materials with a pore width (or diameter) distribution in the range of 2–50 nm for the removal of large dyes from aqueous phases [17–27]. It should be noted that these mesoporous AC materials were mostly produced by chemical activation processes.

Water caltrop (*Trapa natans*) is an aquatic floating plant commonly found in tropical and sub-tropical Asian countries. The pulp within the water caltrop fruit is a popular food because of its richness in starch. However, its outer layer (husk, shell, peel, or pericarps) is stripped off, thus generating water caltrop husk (WCH). This agricultural residue is often discarded in farmlands, or sometimes reused as an organic fertilizer. Due to its lignocellulosic compositions, there are some studies on the reuse of WCH as a biosorbent for dye removal [28–30], and a precursor for producing carbon materials in recent years [31–35]. For example, Kumar et al. [34] investigated the preparation of H_3PO_4-activated carbon from WCH and its removal performance of hexavalent chromium, showing a maximum adsorption capacity of 87.31 mg/g according to the Thomas model.

The adsorbate methylene blue (MB) is a cationic dye, commonly adopted as a probe molecule for determining the specific surface area or adsorption capacity of various materials quickly, including AC, charcoal, graphite, and clay [12,36–38]. It is also used as a chemical indicator, industrial dye, drug (e.g., treatment of malaria), and biological strain [39,40]. However, MB is also a toxic dye, which can result in harmful effects on humans (e.g., diarrhea, vomiting, and cyanosis) and environmental problems [23]. In this regard, the removal of MB as organic pollutant from aqueous solution or effluent is important for environmental protection and human health. Santoso et al. [11] reviewed research on the removal of MB using carbon-based adsorbents (focusing on activated carbon and biochar), and also discussed their structural properties influencing MB adsorption performance.

In a previous study [41], the pore and chemical properties of mesoporous AC produced from coconut shell using a single-step CO_2 activation process were studied, showing that a significant increase in the pore properties of resulting AC was found between 700 and 750 °C. As mentioned above, there is a scarcity of research that has investigated the production of mesoporous AC from WCH using physical activation by gasification gas CO_2. Therefore, this work aims to produce mesoporous AC from WCH by CO_2 activation at lower temperatures (i.e., 750 °C) and longer holding time (i.e., 90 min), and also characterize its pore properties and chemical compositions on the surface. Subsequently, the resulting AC was used to evaluate its removal performance of MB from the aqueous solution under various adsorption conditions.

2. Materials and Methods

2.1. Materials

The starting material (i.e., WCH) for producing mesoporous AC was obtained from a local farmers' association at Guantian District. The sun-dried WCH was first milled and then sieved to obtain particle sizes in the range of 0.420–0.841 mm. The pretreatment of WCH and its thermochemical properties (including proximate analysis, elemental analysis, calorific value, and thermogravimetric analysis) have been described in the previous study [42]. The dried WCH sample with average particle size of 0.63 mm (i.e., passed through mesh No. 20 and retained on mesh No. 40) was used in the physical activation experiments. In this work, the adsorbate MB, which was purchased from Merck Co., was modeled as a toxic pollutant for determining the adsorption capacity of the resulting AC in aqueous solution.

2.2. Physical Activation Experiments

The procedures for the preparation of AC from biomass precursor have been described in the previous study [41]. A vertical electric heating tube reactor (length 80 cm, inner

diameter 10 cm) with a mesh-made sample holder was used to perform the carbonization-activation experiments. In order to produce mesoporous AC, the single-step physical activation experiments were performed in triplicate as follows: the temperature of WCH precursor (about 5 g) was increased to 500 °C at a heating rate of about 10 °C/min under the flow of 500 cm^3/min (N_2). The prepared charcoal was subsequently activated by a gasification gas (CO_2) of 50 cm^3/min under the desired conditions (i.e., activation temperature of 750 °C for holding 90 min). The yield of resulting AC (WCH-AC) was found to be about 10%. Before determining the pore properties of resulting AC (WCH-AC), the product sample was dried at about 105 °C overnight.

2.3. Characterization of Resulting Activated Carbon

The determinations of pore properties for the resulting AC (WCH-AC) were measured at −196 °C by using the ASAP-2020 porosimetry system (Micromeritics Co., Norcross, GA, USA). Using the N_2 adsorption–desorption isotherms obtained, the pore properties, including specific surface area, pore volume, pore size distribution, and average pore size (or width), can be calculated by the corresponding methods or models [13]. For example, the Brunauer-Emmett-Teller (BET) method was used to obtain the so-called BET surface area, which was determined in the relative pressure (P/P_0) range of 0.05–0.30. The micropore surface area and micropore volume were estimated from the *t*-method [13]. Accordingly, the mesopore volume was obtained from total pore volume minus micropore volume. In addition, the modified Kelvin equation using the Harrett–Joyner–Halenda method served as the basis for the analysis of pore size distribution [13]. Based on the helium displacement method, the true densities of resulting AC were determined by the AccuPyc-1340 pycnometer (Micromeritics Co., Norcross, GA, USA). The calculations of other pore properties like particle density and average pore width are referred to in the previous study [43]. The textural microstructures and elemental compositions of resulting AC on the surface were observed by the S-3000N scanning electron microscopy – energy dispersive X-ray spectroscopy (SEM-EDS) (Hitachi Co., Tokyo, Japan). Prior to the SEM-EDS analysis, the sample was plated by the E1010 ion sputter (Hitachi Co., Tokyo, Japan) to form a thin film with conductive gold.

2.4. Experiments of Adsorption Performance

The adsorption experiments for the MB removal from the water solution were similar to the previous study [41]. In this work, the data on the adsorption capacity of MB in the solution (2 L) were determined at the fixed conditions of 25 °C and 200 rpm. The determining process parameters included initial concentrations (i.e., 5, 10, 15, and 20 mg/L), WCH-AC adsorbent dosages (i.e., 0.1, 0.3, and 0.5 g/2 L) and initial pH values (i.e., 3.0, 7.0, and 11.0). For each adsorption experiment, an aliquot solution (about 15 cm^3) was drawn out at specified intervals (i.e., 1, 5, 10, 20, 30, 40, 50, and 60 min). The U-3900 UV/Visible spectrophotometer (Hitachi Co., Tokyo, Japan) was used to analyze the residual MB concentration (i.e., C_t), which was measured at the wavelength of 664 nm.

3. Results and Discussion

3.1. Pore Properties of Resulting Activated Carbon

As listed in Table 1, the pore properties of resulting AC (WCH-AC), including surface area, pore volume, average pore diameter, densities, and porosity were determined in the present study. By comparison, the BET surface area (i.e., 810.5 m^2/g) of WCH-AC was slightly larger than that of commercial AC (i.e., 660 m^2/g) [42]. In addition, this surface area was comparable to other studies on WCH-AC. In the work by Hsu et al. [33], the authors activated the microporous WCH biochar with ZnO and KOH at 900 °C, showing a BET surface area in the range of 1175–1537 m^2/g. In the study by Kumar et al. [34], the BET surface area and *t*-plot micropore volume of WCH-AC by H_3PO_4-activation were 782.89 m^2/g and 0.134 cm^3/g, respectively. Based on the data in Table 1, the ratio of micropore surface area to BET surface area was close to 0.76, which is also consistent with

the ratio of micropore volume to total pore volume (i.e., 0.71). Therefore, the mesopore volume with pore diameter ranging from 2.0 nm to 50.0 nm could be estimated by subtracting the micropore volume from the total pore volume. Although the resulting AC (WCH-AC) is mainly a microporous carbon material, it still featured a mesoporosity of at least 20% or more. Figure 1 depicts its N_2 adsorption and desorption isotherms at −196 °C. From the very high potential for adsorption, the type I isotherms appeared in WCH-AC due to its microporous structure (i.e., pore diameter < 2 nm) [44], which is indicative of micropore filling at P/P_0 less than 0.05. With increases in P/P_0, the so-called hysteresis loop takes place in the WCH-AC, exhibiting adsorbate (i.e., nitrogen molecule) filling by capillary condensation in mesoporous solids (adsorption isotherm), but differing from that of mesopore emptying (desorption isotherm). It can be seen that the data were in accordance with mesopore volume and average pore diameter (0.130 cm^3/g and 2.17 nm, respectively, as listed in Table 1). More consistently, the pore size distribution of WCH-AC had two peaks as shown in Figure 2. One appeared as a narrow curve with the pores with less than 2 nm (micropores), but another was observed at ca. 4 nm (mesopores). Herein, the average pore size of WCH-AC was estimated by its BET surface area and total pore volume assuming cylindrical geometry in all pores [45].

Table 1. Pore properties of resulting activated carbon (WCH-AC).

Property	Value [a]
Single point surface area (m^2/g) [b]	790.8 ± 42.5
BET surface area (m^2/g) [c]	810.5 ± 2 5.7
Langmuir surface area (m^2/g)	1198.5 ± 38.6
Micropore surface area (m^2/g) [d]	618.9 ± 16.6
External surface area (m^2/g) [e]	191.6 ± 19.6
Total pore volume (cm^3/g) [f]	0.441 ± 0.024
Micropore volume (cm^3/g) [d]	0.311 ± 0.013
Pore diameter (Å) [g]	21.7 ± 0.8
True density (g/cm^3) [h]	1.787
Particle density (g/cm^3) [i]	0.999
Porosity (-) [j]	0.441

[a] Average ± standard deviation (n = 3). [b] Measured at 0.30 of relative pressure (P/P_0). [c] Measured in the relative pressure (P/P_0) range of 0.05-0.30. [d] Determined by the *t*-plot method. [e] Equal to BET surface area minus micropore surface area. [f] Measured at 0.995 of P/P_0. [g] Estimated from the total pore volume and BET surface area. [h] Determined by the helium-displacement measurement. [i] Obtained from the values of total pore volume and true density [45]. [j] Obtained from the values of particle density and true density [45].

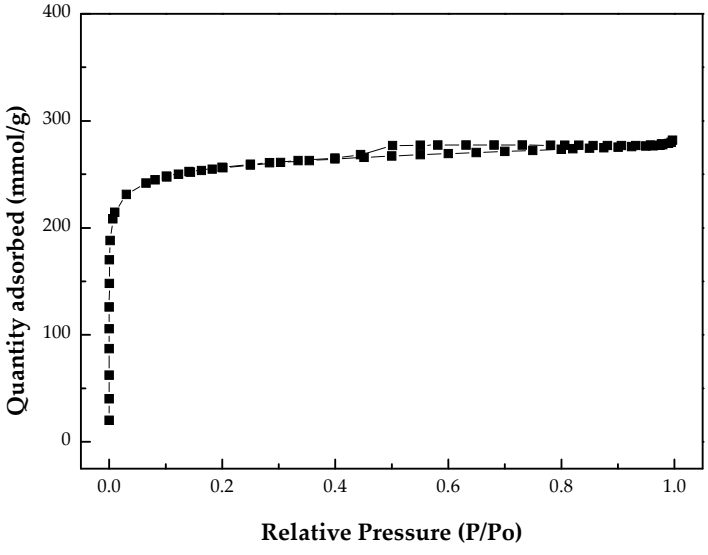

Figure 1. N_2 adsorption–desorption isotherms of resulting activated carbon (WCH-AC).

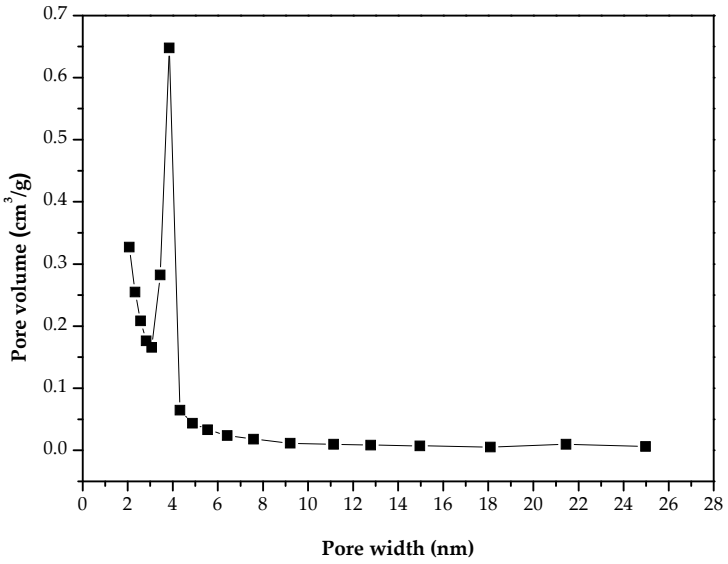

Figure 2. Pore size distribution of resulting activated carbon (WCH-AC).

3.2. SEM-EDS Observations of Resulting Activated Carbon

For confirming the porous microstructures of resulting AC (WCH-AC), the SEM was used to observe its morphological texture with two different magnifications (i.e., 1000 and 3000). As shown in Figure 3, many small pores appeared on the surface of the resulting AC. In addition, the AC also exhibited a rigid frame on the hard surface due to the physical activation of lignocellulosic constituents at a lower temperature (i.e., 750 °C) and longer holding time (i.e., 90 min). Therefore, the porous structure observed by the SEM was highly related to the pore properties, as listed in Table 1. Furthermore, the elemental distributions on the surface of resulting AC were also analyzed by the EDS while observing by the SEM. As illustrated in Figure 4, the main elements, including carbon (85.63 wt%) and oxygen (9.54 wt%), were present in the WCH-AC. It should be noted that the high content of oxygen in the resulting AC was indicative of its richness in functional groups containing oxygen (e.g., carbonyl and hydroxyl) on the surface. The presence of oxygen and other organic elements in surface groups had a profound effect on the adsorption properties of the AC, which is in connection with its slightly polar nature (i.e., hydrophilicity) [12]. Furthermore, some inorganic elements, including potassium (3.69 wt%), sodium (0.39 wt%), and chlorine (0.74 wt%), were found in the resulting AC. They were formed from metal oxides (e.g., K_2O and Na_2O) and metal chlorides (e.g., KCl and NaCl).

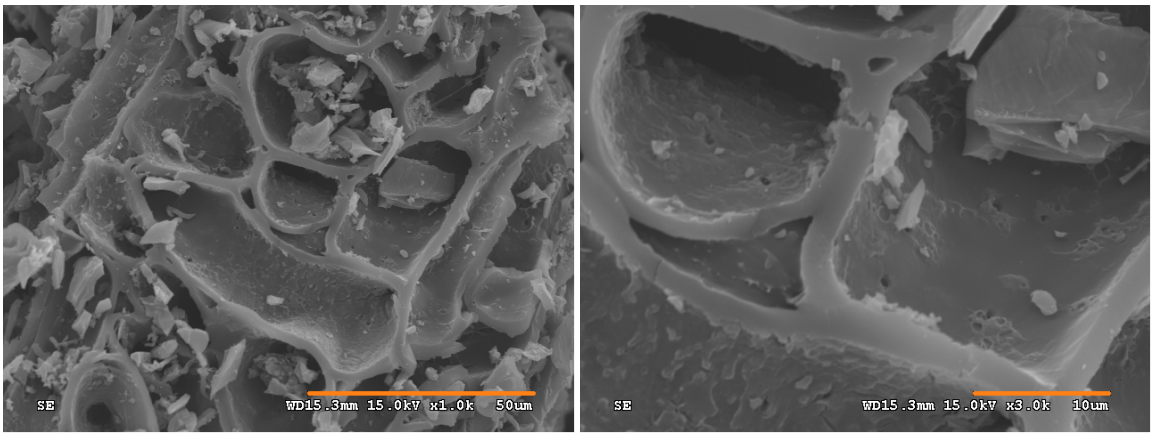

(**a**) (**b**)

Figure 3. SEM images ((**a**) Left: ×1000; (**b**) Right: ×3000) of resulting AC (WCH-AC).

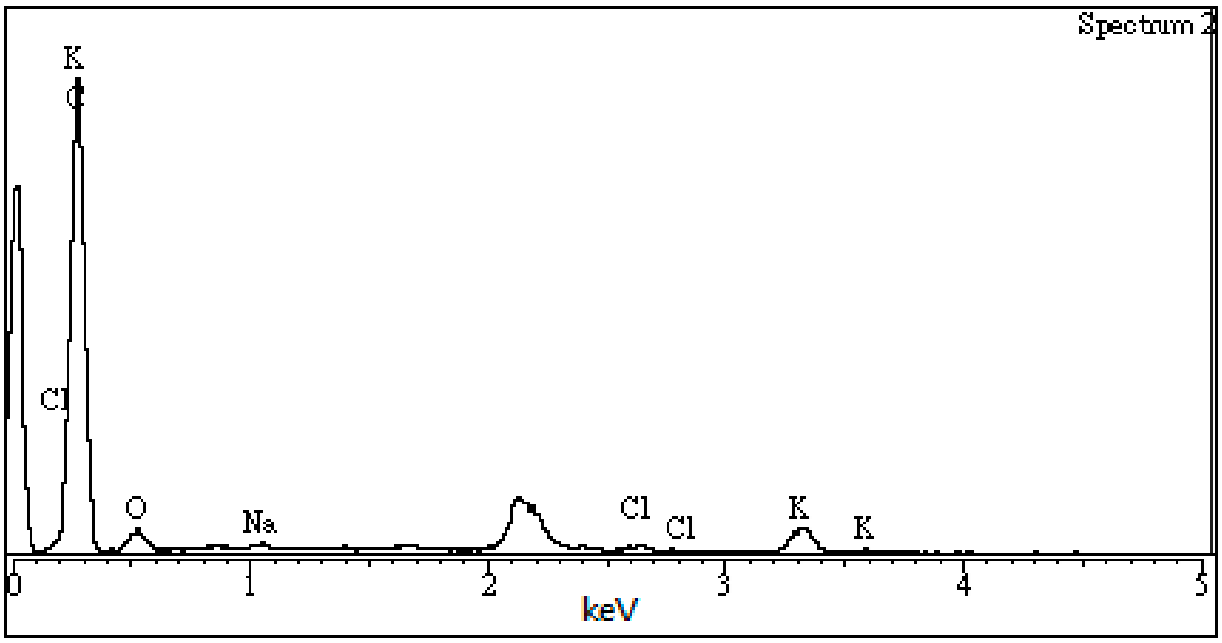

Figure 4. EDS spectra of resulting AC (WCH-AC) and its relative compositions of elements detected.

3.3. Adsorption Performances of Resulting Activated Carbon

Figures 5 and 6 show the variations on residual MB concentration at the specific adsorption conditions under various WCH-AC adsorbent dosages and initial MB concentrations, respectively. It can be seen that the dimensionless residual MB concentration (C_t/C_0) indicated a fast decrease during the limited adsorption time. This indicates a strong interaction between the MB adsorbate and the WCH-AC adsorbent. As mentioned above, the resulting AC should be negatively-polar on its surface. Therefore, a pseudo-second-order model was used to fit the adsorption system with a linear form [46]:

$$t/q_t = 1/(k \times {q_e}^2) + (1/q_e) \times t \quad (1)$$

where q_t is the amount of MB adsorbed at time t (mg/g), q_e is the amount of MB adsorbed at equilibrium (mg/g), and k is the rate constant of this model (g/(mg.min)). Therefore, the adsorption time ($t_{1/2}$) necessary to adsorb half of the adsorption amount of MB at equilibrium ($q_e/2$) by the WCH-AC adsorbent was obtained as follows:

$$t_{1/2} = 1/(k \times q_e) \quad (2)$$

Table 2. Pseudo-second-order model parameters for MB adsorption onto WCH-AC at various WCH-AC dosages. [a]

Adsorbent Dosage (g/2 L)	k (g/(mg.min))	q_e (mg/g)	Correlation Coefficient	$t_{1/2}$ (min)	h (mg/(g.min))
0.1	0.0012	126.58	0.986	6.58	19.23
0.3	0.0147	68.03	1.000	1.00	68.03
0.5	0.1442	40.16	1.000	0.17	232.57

[a] Process conditions: initial MB concentration = 10 mg/L, initial pH = 7.0.

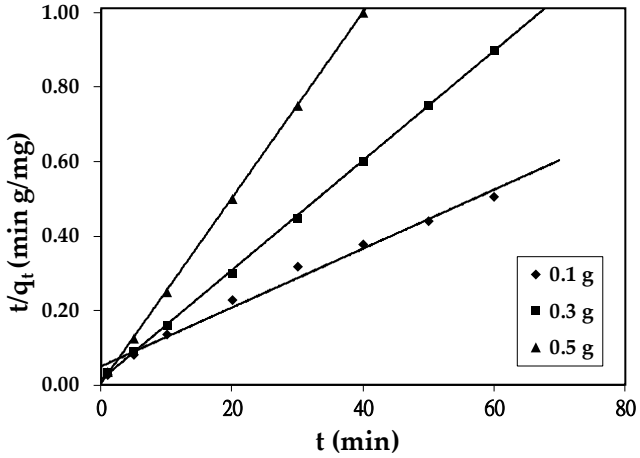

Figure 5. Variations of dimensionless concentration (C_t/C_0) vs. time under various WCH-AC dosages (initial MB concentration = 10 mg/L, initial pH = 7.0); symbols: experimental data, full lines: obtained from the pseudo-second-order model parameters (Table 2).

Table 3. Pseudo-second-order model parameters for MB adsorption onto WCH-AC at various initial MB concentrations. [a]

Initial MB Concentration (mg/L or ppm)	k (g/(mg.min))	q_e (mg/g)	Correlation Coefficient	$t_{1/2}$ (min)	h (mg/(g.min))
5	0.1625	33.44	1.000	0.18	181.71
10	0.0147	68.03	1.000	1.00	68.03
15	0.0024	104.17	0.998	4.00	26.04
20	0.0016	125.00	0.994	5.00	25.00

[a] Process conditions: WCH-AC dosage = 0.3 g/2L, initial pH = 7.0.

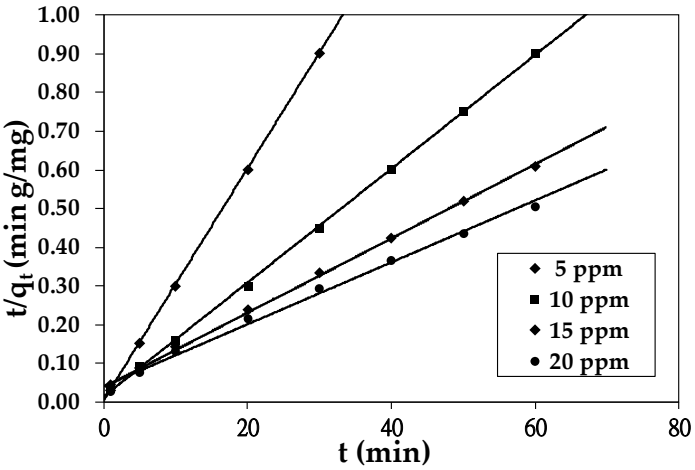

Figure 6. Variations of dimensionless concentration (C_t/C_0) vs. time under various initial MB concentrations (WCH-AC dosage = 0.3 g/2 L, initial pH = 7.0); symbols: experimental data, full lines: obtained from the pseudo-second-order model parameters (Table 3).

In addition, the initial adsorption rate (h) was obtained by the equation [47,48]:

$$h = k \times q_e{}^2 \quad (3)$$

By using the model fitting, the values of the adsorption parameters for the AC-MB system were summarized in Table 2, Table 3, and Table 4, which correspond to the processes'

parameters of adsorbent dosage, initial MB concentration, and pH, respectively. With high correlation coefficients (>0.98), the adsorption of MB into WCH-AC followed this kinetic model well. Regarding the discussion on the relationships between the values of the fitted model parameters (i.e., q_e, k, and h) and process parameters (i.e., adsorbent dosage and C_0), this has been elucidated in previous studies [43]. The data in Table 4 indicates an important significance. At the acidic solution, the surface of resulting AC was protonized by excessive protons. As a consequence, the cationic dye (i.e., MB) was repelled more from the positively charged surface because of the repulsive force [49]. In contrast, the surface of resulting AC was prone to lose the protons at a higher basicity, thus resulting in the negatively charged surface for adsorbing the adsorbate MB preferably due to the electrostatic attraction.

Table 4. Pseudo-second-order model parameters for MB adsorption onto WCH-AC at three different pH values. [a]

Initial pH	k (g/(mg.min))	q_e (mg/g)	Correlation Coefficient	$t_{1/2}$ (min)	h (mg/(g.min))
3	0.0101	68.97	1.000	1.44	48.04
7	0.0147	68.03	1.000	1.00	68.03
11	0.0207	69.93	1.000	0.69	101.23

[a] Process conditions: WCH-AC dosage = 0.3 g/2L, initial concentration = 10 mg/L.

4. Conclusions

In this study, the pore properties and adsorption performances of the mesoporous AC from water caltrop husk prepared at lower temperature (i.e., 750 °C) and longer holding time (i.e., 90 min) are summarized as follows:

- The resulting AC possessed a mesoporous feature with the BET specific surface area of 810.5 m^2/g and mesopore volume of 0.13 cm^3/g, which are superior to commercial AC products.
- Due to its fast adsorption rate and maximal adsorption capacity fitted by the model (126.6 mg/g), the mesoporous carbon material could be used as an excellent adsorbent for liquid-phase removal of MB.
- The pseudo-second-order model is well suited for describing the adsorption system, which includes the cationic adsorbate and the resulting AC with hydrophilicity of oxygen surface groups.

Author Contributions: Conceptualization, W.-T.T.; methodology, Y.-Q.L.; validation, Y.-Q.L.; data curation, Y.-Q.L.; formal analysis, Y.-Q.L.; writing—original draft preparation, W.-T.T.; writing—review and editing, W.-T.T. All authors have read and agreed to the published version of the manuscript.

Funding: This research received no external funding.

Institutional Review Board Statement: Not applicable.

Informed Consent Statement: Not applicable.

Acknowledgments: The SEM-EDS observations were assisted by the Instrument Center at National Pingtung University of Science and Technology.

Conflicts of Interest: The authors declare no conflict of interest.

References

1. Teodosiu, C.; Gilca, A.F.; Barjoveanu, G.; Fiore, S. Emerging pollutants removal through advanced drinking water treatment: A review on processes and environmental performances assessment. *J. Clean. Prod.* **2018**, *197*, 1210–1221. [CrossRef]
2. Jeirani, Z.; Niu, C.H.; Soltan, J. Adsorption of emerging pollutants on activated carbon. *Rev. Chem. Eng.* **2017**, *33*, 491–522. [CrossRef]
3. Al-Ghouti, M.A.; Al-Kaabi, M.A.; Ashfag, M.Y.; Da'na, D.A. Produced water characteristics, treatment and reuse: A review. *J. Water Process Eng.* **2019**, *28*, 222–239. [CrossRef]

4. Tsai, W.T.; Chang, C.Y.; Ho, C.Y.; Chen, L.Y. Adsorption properties and breakthrough model of 1,1-dichloro-1-fluoroethane on activated carbons. *J. Hazard. Mater.* **1999**, *69*, 53–66. [CrossRef]
5. Loannidou, O.; Zabaniotou, A. Agricultural residues as precursors for activated carbon production—A review. *Renew. Sust. Energy Rev.* **2007**, *11*, 1966–2005. [CrossRef]
6. Paraskeva, P.; Kalderis, D.; Diamadopoulos, E. Production of activated carbon from agricultural by-products. *J. Chem. Technol. Biotechnol.* **2008**, *83*, 581–592. [CrossRef]
7. Alslaibi, T.M.; Abustan, I.; Ahmad, M.A.; Foul, A.A. A review: Production of activated carbon from agricultural byproducts via conventional and microwave heating. *J. Chem. Technol. Biotechnol.* **2013**, *88*, 1183–1190. [CrossRef]
8. Yahya, M.A.; Al-Qodah, Z.; Ngah, C.W.Z. Agricultural bio-waste materials as potential sustainable precursors used for activated carbon production: A review. *Renew. Sust. Energy Rev.* **2015**, *46*, 218–235. [CrossRef]
9. Gonzalez-Garcia, P. Activated carbon from lignocellulosics precursors: A review of the synthesis methods, characterization techniques and applications. *Renew. Sust. Energy Rev.* **2018**, *82*, 1393–1414. [CrossRef]
10. Qureshi, U.A.; Hameed, B.H.; Ahmed, M.J. Adsorption of endocrine disrupting compounds and other emerging contaminants using lignocellulosic biomass-derived porous carbons: A review. *J. Water Process Eng.* **2020**, *38*, 101380. [CrossRef]
11. Santoso, E.; Ediati, R.; Kusumawati, Y.; Bahruji, H.; Sulistiono, D.O.; Prasetyoko, D. Review on recent advances of carbon based adsorbent for methylene blue removal from waste water. *Mater. Today Chem.* **2020**, *16*, 100233. [CrossRef]
12. Marsh, H.; Rodriguez-Reinoso, F. *Activated Carbon*; Elsevier: Amsterdam, The Netherlands, 2006.
13. Lowell, S.; Shields, J.E.; Thomas, M.A.; Thommes, M. *Characterization of Porous Solids and Powders: Surface Area, Pore Size and Density*; Springer: Dordrecht, The Netherlands, 2006.
14. Ruthven, D.M. *Principles of Adsorption and Adsorption Processes*; John Wiley & Sons: New York, NY, USA, 1984.
15. Hsieh, C.T.; Teng, H. Influence of mesopore volume and adsorbate size on adsorption capacities of activated carbons in aqueous solutions. *Carbon* **2000**, *38*, 863–869. [CrossRef]
16. Piai, L.; Dykstra, J.E.; Adishakti, M.G.; Blockland, M.; Langenhoff, A.A.M.; van der Wal, A. Diffusion of hydrophilic organic micropollutants in granular activated carbon with different pore sizes. *Water Res.* **2019**, *162*, 518–527. [CrossRef] [PubMed]
17. Hu, Z.; Srinivasan, M.P.; Ni, Y. Preparation of mesoporous high-surface-area activated carbon. *Adv. Mater.* **2000**, *12*, 62–65. [CrossRef]
18. Macedo, J.S.; Junior, N.B.C.; Almeida, L.E.; Vieira, E.F.S.; Cestari, A.R.; Gimenez, I.F.; Carreno, N.L.V.; Barreto, L.S. Kinetic and calorimetric study of the adsorption of dyes on mesoporous activated carbon prepared coir dust. *J. Colloid Interface Sci.* **2006**, *298*, 515–522. [CrossRef]
19. Gao, J.; Kong, D.; Wang, Y.; Wu, J.; Sun, S.; Xu, P. Production of mesoporous activated carbon from tea fruit peel residues and its evaluation of methylene blue removal from aqueous solutions. *BioResources* **2013**, *8*, 2145–2160. [CrossRef]
20. Salman, J.M. Preparation of mesoporous-activated carbon from branches of pomegranate trees: Optimization on removal of methylene blue using response surface methodology. *J. Chem.* **2013**, 489670. [CrossRef]
21. Yu, L.; Luo, Y.M. The adsorption mechanism of anionic and cationic dyes by Jerusalem artichoke stalk-based mesoporous activated carbon. *J. Environ. Chem. Eng.* **2014**, *2*, 220–229. [CrossRef]
22. Islam, A.A.; Ahmed, M.J.; Khanday, W.A.; Asif, M.; Hameed, B.H. Mesoporous activated carbon prepared from NaOH activation of rattan (*Lacosperma secundiflorum*) hydrochar for methylene blue removal. *Ecotoxicol. Environ. Saf.* **2017**, *138*, 279–285. [CrossRef]
23. Jawad, A.H.; Rashid, R.A.; Ismail, K.; Sabar, S. High surface area mesoporous activated carbon developed from coconut leaf by chemical activation with H_3PO_4 for adsorption of methylene blue. *Desalin. Water Treat.* **2017**, *74*, 326–335. [CrossRef]
24. Marrakchi, F.; Ahmed, M.J.; Khanday, W.A.; Asif, M.; Hameed, B.H. Mesoporous-activated carbon prepared from chitosan flakes via single-step sodium hydroxide activation for the adsorption of methylene blue. *Int. J. Biol. Macromol.* **2017**, *98*, 233–239. [CrossRef]
25. Wongcharee, S.; Aravinthan, V.; Erdei, L.; Sanongraj, W. Mesoporous activated carbon prepared from macadamia nut shell waste by carbon dioxide activation: Comparative characterization and study of methylene blue removal from aqueous solution. *Asian-Pac. J. Chem. Eng.* **2018**, *13*, e2179. [CrossRef]
26. Khasri, A.; Bello, O.S.; Ahmad, M.A. Mesoporous activated carbon from *Pentace* species sawdust via microwave-induced KOH activation: Optimization and methylene blue adsorption. *Res. Chem. Intermed.* **2018**, *44*, 5737–5757. [CrossRef]
27. Boudia, R.; Mimanne, G.; Benhabib, K.; Pirault-Roy, L. Preparation of mesoporous activated carbon from date stones for the adsorption of Bemacid Red. *Water Sci Technol.* **2019**, *79*, 1357–1366. [CrossRef] [PubMed]
28. Khan, T.A.; Nazir, M.; Khan, E.A. Adsorptive removal of rhodamine B from textile wastewater using water chestnut (*Trapa natans L.*) peel: Adsorption dynamics and kinetic studies. *Toxicol. Environ. Chem.* **2013**, *95*, 919–931. [CrossRef]
29. Rehman, R.; Salariya, B.; Mitu, L. Batch scale adsorptive removal of brilliant green dye using *Trapa natans* peels in cost effective manner. *Rev. Chim.* **2016**, *67*, 1333–1337.
30. Kumar, S.; Naryanasamy, S.; Venkatesh, R.P. Removal of Cr (VI) from synthetic solutions using water caltrop shell as a low-cost biosorbent. *Sep. Sci. Technol.* **2019**, *54*, 2783–2799. [CrossRef]
31. Rao, L.L.; Liu, S.F.; Wang, L.L.; Ma, C.D.; Wu, J.Y.; An, L.Y.; Hu, X. N-doped porous carbons from low-temperature and single-step sodium amide activation of carbonized water chestnut shell with excellent CO_2 capture performance. *Chem. Eng. J.* **2019**, *359*, 428–435. [CrossRef]

32. Wang, P.; Fan, L.; Yan, L.; Shi, Z. Low-cost water caltrop shell-derived hard carbons with high initial coulombic efficiency for sodium-ion battery anodes. *J. Alloys Compd.* **2019**, *775*, 1028–1035. [CrossRef]
33. Hsu, C.H.; Pan, Z.B.; Chen, C.R.; Wei, M.X.; Chen, C.A.; Lin, H.P.; Hsu, C.H. Synthesis of multiporous carbons from the water caltrop shell for high-performance supercapacitors. *ACS Omega* **2020**, *5*, 10626–10632. [CrossRef]
34. Kumar, S.; Patra, C.; Naryanasamy, S.; Rajaraman, P.V. Performance of acid-activated water caltrop (*Trapa natans*) shell in fixed bed column for hexavalent chromium removal from simulated wastewater. *Environ. Sci. Pollut. Res.* **2020**, *27*, 28042–28052. [CrossRef] [PubMed]
35. Yin, W.J.; Zhang, Z.H.; Liu, T.C.; Xu, J.; Xiao, S.Z.; Xu, Y. N-doped animal keratin waste porous biochar derived from *Trapa natans* husks. *Materials* **2020**, *13*, 987. [CrossRef] [PubMed]
36. Kaewprasit, C.; Hequet, E.; Abidi, N.; Gourlot, J.P. Application of methylene blue adsorption to cotton fiber specific surface area measurement: Part I. methodology. *J. Cotton Sci.* **1998**, *2*, 164–173.
37. Chen, G.; Pan, J.; Han, B.; Yan, H. Adsorption of methylene blue on montmorillonite. *J. Dispers. Sci. Technol.* **1999**, *20*, 1179–1187. [CrossRef]
38. Hegyesi, N.; Vad, R.T.; Pukanszky, B. Determination of the specific surface area of layered silicates by methylene blue adsorption: The role of structure, pH and layer charge. *Appl. Clay Sci.* **2017**, *146*, 50–55. [CrossRef]
39. Jia, P.; Tan, H.; Liu, K.; Gao, W. Removal of methylene blue from aqueous solution by bone char. *Appl. Sci.* **2018**, *8*, 1903. [CrossRef]
40. Lu, G.; Nagbanshi, M.; Goldau, N.; Mendes Jorge, M.; Meissner, P.; Jahn, A.; Mockenhaupt, F.P.; Muller, O. Efficacy and safety of methylene blue in the treatment of malaria-a systematic review. *BMC Med.* **2018**, *16*, 59. [CrossRef]
41. Tsai, W.T.; Jiang, T.J. Mesoporous activated carbon produced from coconut shell using a single-step physical activation process. *Biomass Conver. Biorefin.* **2018**, *8*, 711–718. [CrossRef]
42. Tsai, W.T.; Lin, Y.Q.; Tsai, C.H.; Chung, M.H.; Chu, M.H.; Huang, H.J.; Jao, Y.H.; Yeh, S.I. Conversion of water caltrop husk into biochar by torrefaction. *Energy* **2020**, *195*, 116967. [CrossRef]
43. Tsai, W.T.; Huang, P.C.; Lin, Y.Q. Reusing cow manure for the production of activated carbon using potassium hydroxide (KOH) activation process and its liquid-phase adsorption performance. *Processes* **2019**, *7*, 737. [CrossRef]
44. Gregg, S.J.; Sing, K.S.W. *Adsorption, Surface Area, and Porosity*; Academic Press: London, UK, 1982.
45. Smith, J.M. *Chemical Engineering Kinetics*, 3rd ed.; McGraw-Hill: New York, NY, USA, 1981.
46. Ho, Y.S.; Chiang, C.C.; Hsu, Y.C. Sorption kinetics for dye removal from aqueous solution using activated clay. *Sep. Sci. Technol.* **2001**, *36*, 2473–2488. [CrossRef]
47. Hamadi, N.K.; Swaminathan, S.; Chen, X.D. Adsorption of paraquat dichloride from aqueous solution by activated carbon derived from used tires. *J. Hazard. Mater.* **2004**, *B112*, 133–141. [CrossRef] [PubMed]
48. Paska, O.M.; Pacurariu, C.; Muntean, S.G. Kinetic and thermodynamic studies on methylene blue biosorption using corn-husk. *RSC Adv.* **2014**, *4*, 62621–62630. [CrossRef]
49. Zaini, M.A.A.; Okayama, R.; Machida, M. Adsorption of aqueous metal ions on cattle-manure-compost based activated carbons. *J. Hazard. Mater.* **2009**, *170*, 1119–1124. [CrossRef] [PubMed]